Konya Mühendislik Bilimleri Dergisi, c. 12, s. 1, 150-161, 2024
Konya Journal of Engineering Sciences, v. 12, n. 1, 150-161, 2024
ISSN: 2667-8055 (Electronic)
DOI: 10.36306/konjes.1379888

ADSORPTION OF MALACHITE GREEN INTO POTATO PEEL: NONLINEAR ISOTHERM AND KINETIC

[1]İlhan KÜÇÜK, [2]Halil BİÇİÇİ

[1] *Muş Alparslan University, Rektorship, Muş, TÜRKİYE*
[2] *Muş Alparslan University, Applied Sciences Faculty, Muş, TÜRKİYE*
[1] i.kucuk@alparslan.edu.tr, [2] hbicici17@gmail.com

(Received: 23.10.2023; Accepted in Revised Form: 01.02.2024)

ABSTRACT: Potato peels (PPs) were utilized for removal of malachite green (MG) from aqueous solutions. The adsorbent underwent characterization through attenuated total reflection fourier transform infrared spectroscopy (ATR-FTIR), Scanning electron microscope (SEM), point zero charge (pH_{PZC}) X-Ray diffraction (XRD), and Energy dispersive X-ray spectroscopy (EDX). The removal of MG was found to be significantly influenced by pH, temperature, contact time, and initial concentration. Temperature and particle size were determined to have lesser influence compared to other factors. The adsorption process lasted for 120 minutes, with rapid removal occurring within the first 60 minutes. Adsorption kinetics were analyzed using the Elovich, pseudo first order, and pseudo second order models. The pseudo second order model was found to be more suitable for the kinetic study. Isotherm modeling was conducted using the Temkin, Freundlich, and Langmuir isotherms. Due to the exothermic nature of the study, the Freundlich and Langmuir models were found to be highly compatible. The maximum adsorption capacity was determined as 37.8 mg/g at 41°C. ATR-FTIR analysis revealed the involvement of hydroxide and carbonyl groups in the adsorption process. Overall, this study concluded that PPs is promising adsorbent for removal of MG from aqueous solutions.

Keywords: *Raw adsorbent, Malachite green, Adsorption, Nonlinear isotherm-kinetic models, Potato peel*

1. INTRODUCTION

The effluent waste stream from dyeing processes alters water chemistry, damaging aquatic ecosystems. In the past few years, significant damage has been caused by this untreated discharge, which comprises 10-15% of the dyes in the effluent from paper, textile production, leather tanning, food processing industries, and various dyes used in hair colouring products [1]. Dyes are dangerous contaminants as they are toxic, mutagenic, carcinogenic, and non-degradable, and they tend to remain stable in the environment for an extended period [2].

MG is a synthetic triphenylmethane dye that is classified as cationic dye and has the feature of being very water-soluble. MG is often used as a disinfectant in the fish farming sector and in animal husbandry, as an antiseptic and fungicidal agent in humans, and to suppress fungal assaults and protozoan diseases in aquaculture [3]. MG is also frequently used in the cotton, silk, wool, paper, and leather dyeing industries [4]. Despite being widely used in both medicinal and industrial settings, MG has negative impacts on human health and harms the environment. The harmful effects of MG include teratogenesis, carcinogenesis, and mutagenesis, which result in reproductive, immunological, and brain system damage as well as respiratory illnesses [5]. Additionally, the release of MG into the hydrosphere alters photosynthetic activity and lowers sunlight penetration while producing noticeable colouration even at low MG concentrations. The removal of MG from industrial effluents before release into the aquatic environment is therefore becoming an increasing problem [6].

Different methods have been proposed and tested to treat water and remove toxic compounds, including adsorption, ozonation, ultrafiltration, flocculation and oxidation [7]. Among these techniques, adsorption is considered the best approach as it offers several advantages compared to others. It is an effective method with low energy consumption, simple operation, and capable of reducing the

***Corresponding Author:** İlhan KÜÇÜK, i.kucuk@alparslan.edu.tr

concentrations of dye and pharmaceuticals in polluted streams. Using materials with functionalized surfaces is alternative to improve removal efficiency of adsorption for water treatment and purification [8].

There are many studies in the literature related to potato peel [9-11]. These studies generally focus on various industrial applications of potato peel. However, research on the adsorption of malachite green dye by raw potato peel is quite limited. In particular, there is a lack of kinetic studies on the adsorption of malachite green by raw potato peel [12]. Therefore, more detailed and comprehensive studies are needed in this area. The results of these studies can reveal the potential of using potato peel in an environmentally friendly way for the treatment of dyes. Research in this area is of great importance in terms of the disposal of industrial waste and the reduction of environmental pollution.

The objective of this study was to determine capacity of raw adsorbent to adsorb MG. PPs with varying pore sizes were used as the adsorbent. The study investigated various parameters such as particle size, pH, temperature, contact time, and initial concentration. The data obtained from the study were applied to different kinetic and isotherm models to determine results.

2. MATERIAL AND METHODS

Potatoes were purchased from the market located in the Eastern Anatolia Region of Turkey. After being washed multiple times, they were peeled and left to dry in open air. The dried peels were then cut into pieces by hand and shredded with a laboratory blender. The biosorbent was characterized using ATR-FTIR, SEM, pH_{PZC}, XRD and EDX.

During the experiment, we tested the adsorption isotherm at three distinct temperatures: 21°C, 31°C, and 41°C. To conduct the test, we shook 0.05 g of PP (Particle size=0.5<PP<0.425). adsorbent with 50 mL of MG (Figure 1) solution with varying initial concentrations (ranging from 10 to 50 mg/L). After three hours of reaching equilibrium, we analyzed the concentration of MG via UV-Vis (616 nm). The adsorption capacity of adsorbent was calculated through following equation:

Figure 1. Malachite green structure

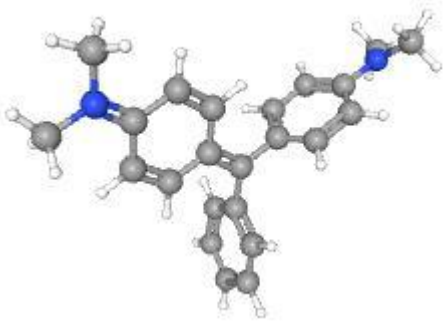

$$q_t = \frac{(C_0 - C_t)V}{w} \quad (1)$$

During the experiment, we conducted a kinetic study to determine the effects of varying initial MG concentrations, temperatures, and particle sizes. To begin with, we mixed a constant adsorbent dose of 0.2 g/L with 200 mL of the MG solution at the desired initial concentration. The resulting mixture was then agitated at a constant speed of 200 rpm for a set amount of time.

The particle size distribution analysis was performed on 100 grams of PP. The PP was washed, dried

in open area, and then ground using a laboratory blender. Six types of Laboratory Test Sieves (ISO 3310-1) ranging from 0.250 mm to 1 mm were used to pass the PP through. The weight of different particle sizes was measured, and a graph was plotted to show the particle size versus the particle amount. The PP was analyzed using ATR-FTIR analysis in Agilent Cary 630 Infrared Spectrophotometer equipped with a spectrum range of 4000-500 cm^{-1}, resolution of 2 cm^{-1}, and particle size of 0.5<PP<0.425 mm to observe different functional groups. The XRD spectrum of the PP was analyzed in a PANalytical Empyrean with a spectrum range of 10-80 2θ, X-ray generator of 4 kW, and particle size of 0.5<PP<0.425 mm to observe crystallization. The SEM (scanning electron microscope model LEO-EVO 40) and EDX (energy dispersive X-ray analysis model Bruker-125 eV) were used to determine the surface morphologies of raw and MG adsorbed PP (particle size = 0.5<PP<0.425 mm).

3. RESULTS AND DISCUSSION

3.1. Characterization of PP

The functional groups in PP adsorbent were identified by analyzing its ATR-FTIR spectrum and its characteristic vibrations. The analysis further supported the adsorption mechanism by demonstrating that the vibrations of functional groups in adsorbents can change when they come into contact with cation ions in dye through various interactions such as covalent bonding, complexation, electrostatic interactions, or hydrogen bonding. The infrared spectra of PP adsorbent before and after adsorption are presented in Figure 2 A.

The ATR-FTIR spectrum in Figure 2 A shows broad peak at 3270 cm^{-1}, confirming presence of free and O-H stretching vibrations of hydroxyl group within the hemicellulose, lignin, and cellulose in adsorbent structure. The vibration observed at 2918 cm^{-1} is attributed to stretching of the C-H bonds in methylene groups and methyl found in adsorbent's polymers such as hemicellulose, lignin, and cellulose [2]. The peak at 1618 cm^{-1} indicates the presence of aromatic compounds in lignin components of adsorbent, and is associated with C-O stretching vibration of ketones and aldehydes, as well as C=C stretching vibration of benzene ring [13]. The peaks at 1021 cm^{-1} and 1318 cm^{-1} correspond to stretching vibrations of hydroxyl and carboxylate group's C-O bonds, respectively, in hemicellulose, cellulose and lignin [14]. The 1409 cm^{-1} peak corresponds to the OH bending vibration, whereas the peak at 1236 cm^{-1} is attributed to stretching vibration of the C-O-C bonds in aryl-alkyl ether linkages and deformation of phenolic OH plane in hemicellulose and cellulose components of lignocellulosic structure of the adsorbent [15]. The 1021 cm^{-1} vibrations can be attributed to primary amine functional groups present on the adsorbent surface, whereas the vibration observed at 1137 cm^{-1} may be linked to stretching of tertiary amine groups. [16]. Lignocellulosic materials contain hydroxyl and carboxylate groups that have been reported to interact with metal ions during adsorption. There are noticeable changes in the frequency spectrum of the adsorbent following adsorption. Some of the bands have an increase in intensity, with one of the most prominent being the O-H, C-O stretching and bending vibrations. This observation provides further evidence that these groups on the surface of the residue are indeed involved in the adsorption interactions [17].

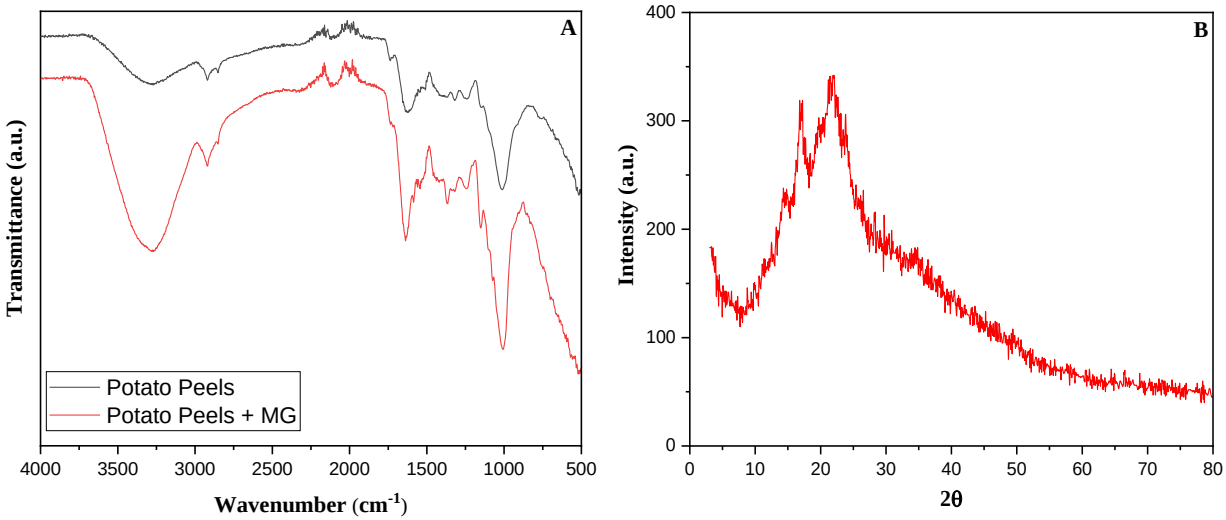

Figure 2. A. ATR-FTIR spectrum of PPs B. XRD spectrum of PPs

XRD patterns of PPs are shown in Figure 2 B, which display the characteristic peaks of cellulosic materials. The absence of sharp peaks confirms the amorphous nature of PPs. There are only four peaks observed at approximately 14°, 18°, 21°, and 34°, corresponding to the reflection from the 101, 101, 200, and 004 planes, respectively. These peaks indicate the structure's presence of hemicellulose, lignin, and cellulose [18].

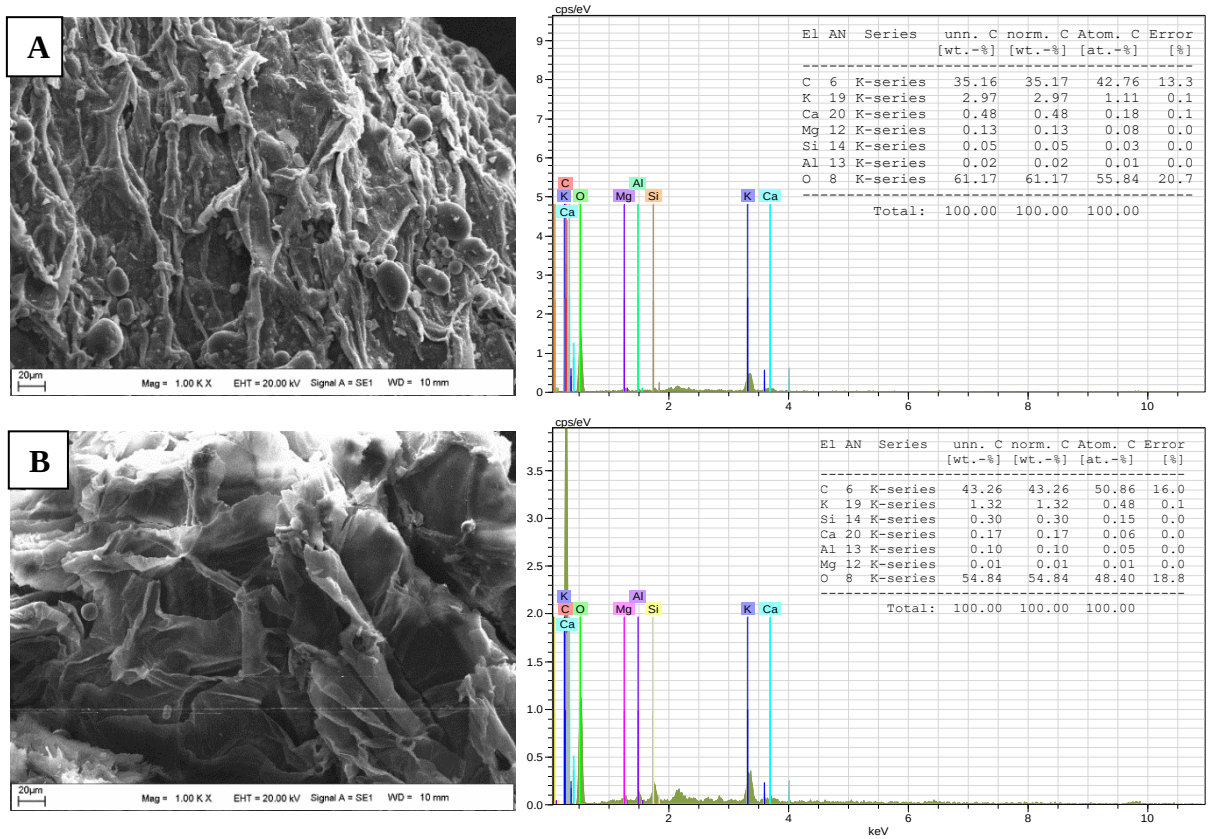

Figure 3. A. Before MG adsorption of PPs **B.** After MG adsorption of PPs

Figure 3 A shows SEM micrograph of PP adsorbent, indicating presence of uneven crevices that likely play significant role in transport of MG during adsorption. Figure 3 B illustrates the morphology of the

structure following adsorption. It is evident that the structure, which previously had cracks, becomes flatter after adsorption. The relative compositions of chemical elements present in an adsorbent can be analyzed by utilizing energy-dispersive X-ray coupled with the SEM instrument. After analysis, the carbon level has increased from 35.16 to 43.26, while the oxygen level has decreased from 61.17 to 54.84. Furthermore, the changes in other elements are shown in Figure 3. EDX results provide evidence of increased carbon, indicating that the structure effectively adsorbs MG.

3.2. Adsorption of MG

Figure 4 A illustrates the distribution of particle sizes. The weight of each class is depicted in relation to the diameter of the particles. Three specific ranges of particle sizes have been chosen: < 0.25, 0.5-0.425, and 1-0.85. The pH of aqueous solution is crucial factor that affects sorption of dyes. It influences speciation of ions in the solution and, consequently, determines types of ions present at specific concentrations of hydroxyl or hydrogen ions [19]. This, in turn, determines the effectiveness of adsorbents in removing these ions. At a higher pH, PP was more effective in removing MG, as shown in Figure 4 C. When the pH value of the aqueous solution is acidic, the removal efficiency was lower. This is because the positively charged CV ions are repelled by the protonation of hydroxyl and carbonyl groups on the surface of lignocellulosic material, which negatively affects the removal efficiency. However, as the pH increases, the negatively charged surface of the lignocellulosic material changes its charge, making it easier to remove positively charged CV ions from the water. This claim is supported by the analysis of pH_{pzc}, which

was determined to be 6.35 (Figure 4 B, T=21°C, PP=0.05g, $C_{0\ NaCl}$= 0.1 M, Particle size=0.5<PP<0.425), indicating that surface of this adsorbent is positively charged below this pH.

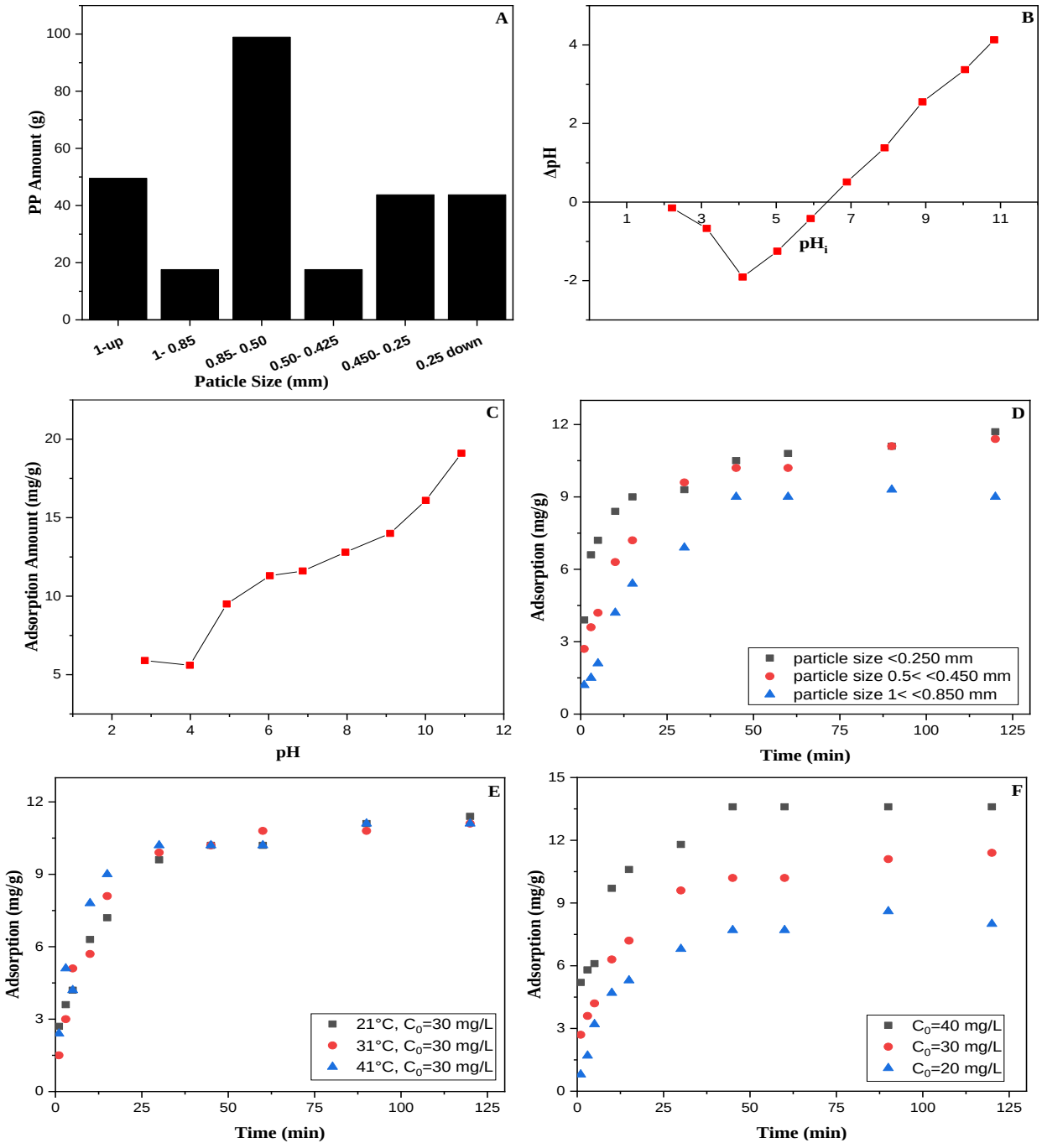

Figure 4. A. Particle size of PPs B. pH_{pzc} of PPs C. Effect of pH on MG adsorption D. Effect of particle size on MG adsorption E. Effect of temperature on MG adsorption F. Effect of contact time and initial concentration on MG adsorption

Size of adsorbent particles greatly affects their capacity to adsorb pollutants. Increasing the particle size usually leads to a decrease in adsorptive properties due to a reduced surface area. Conversely, decreasing the particle size enhances adsorptive properties by increasing the surface area. However, significantly reducing particle size may result in less efficient and environmentally friendly remediation techniques. Drawbacks of extremely small particle sizes include reduced adsorbent yield and rigidity, as

well as increased adsorption process costs [20]. Therefore, optimizing particle size is necessary for each unique remediation case. To investigate this, MG batch adsorption experiments were conducted using three particle sizes (1.00–0.850, 0.50–0.450, and 0.250– down mm). Figure 4 D (T=21°C, pH=5, C0=30 mg/L, pp=0.05 g) displays removals of MB by three adsorbents at different particle sizes. It was observed that the adsorption decreases as the particle size increases, compared to the adsorption at smaller particle sizes. The removal efficiency of PP for MG from aqueous solutions was investigated at three different temperatures: 21, 31, and 41°C. Figure 4 E shows the variation in adsorption capacity of PP for MG over time at these temperatures (pH=5, C_0=30mg/L, Particle size=0.5<PP<0.425). Initially, adsorption tended to decrease as temperature increased. The adsorption capacity at low temperature in the first minute was 2.7 mg/g. However, it decreased to 1.5 mg/g with increasing temperature. Although the adsorption values equalize over time, there are partial decreases in adsorption observed after 120 minutes at higher temperatures. At 21°C, the adsorption amount was 11.4 mg/g, while at 41°C, it was 11.1 mg/g. This indicates that the system undergoes an exothermic adsorption [21]. The decrease in adsorption at higher temperatures may be attributed to increased thermal energy of system. As the temperature rises, the kinetic energy of the adsorbate molecules also increases, leading to a greater tendency for desorption to occur. This phenomenon is commonly observed in exothermic adsorption processes, where the release of heat during adsorption can result in a decrease in adsorption capacity over time.

The adsorption of MG dye over time is shown in Figure 4 F. Initially, the adsorption was rapid, with around 50% of the dye being adsorbed within the first 5 minutes. As the contact time between the adsorbent and adsorbate increased, uptake of MG gradually increased up to 45 minutes, reaching a maximum removal rate. This initial fast adsorption rate may be attributed to abundance of active sites and pores on surface of adsorbent [22]. However, as the adsorption process continued, the accumulation of dye molecules on surface hindered diffusion into pores, resulting in slower adsorption rate. The effect of initial metal concentration on adsorption capacity of PGP was investigated for concentration values of 20, 30, and 40 mg/L, as illustrated in Figure 4 F (T=21°C, pH=5, PP=0.05g, Particle size=0.5<PP<0.425). Adsorption capacity rises from 8 mg/g to 13.6 mg/g as initial MG concentration increases from 20 mg/L to 40 mg/L, until it reaches a constant value where no more MG can be eliminated. The increase in adsorption capacity is attributed to high concentration of MG ions in the concentrated solution. The saturation point is reached when concentration of MG ions in solution becomes too high for further adsorption onto PP. At this point, the adsorption capacity remains constant since no more MG can be removed from the solution. This observation indicates that the adsorption process relies on the initial MG concentration. Higher initial MG concentrations provide a larger quantity of MG ions accessible for adsorption, resulting in an enhanced adsorption capacity of PP. Understanding the relationship between initial MG concentration and adsorption capacity is crucial in assessing the effectiveness of PP as a potential adsorbent for MG removal.

3.2.1. Adsorption isotherm and kinetic

Adsorption is the binding or adherence of a substance or molecule to a surface, a process that plays a crucial role in various industrial applications such as catalysis, water and gas purification, and pharmaceutical production. Adsorption isotherms, which are mathematical models of the adsorption process, are used to describe the adsorption equilibrium state [23].

The Temkin, Freundlich, and Langmuir models are commonly used adsorption isotherm models. These models provide a mathematical expression of the adsorption process and are used to determine its agreement with experimental data.

The Langmuir model describes monolayer adsorption, relating the number of adsorbed molecules on surface of adsorbent, the number of vacant places on surface, and the equilibrium state of adsorption. The Langmuir isotherm equation calculates the adsorption capacity and rate [24]. The Freundlich model explains multilayer adsorption by expressing the relationship between the number of active sites on surface of adsorbent and concentration of adsorbent. The Freundlich isotherm equation is non-linear expression of adsorption process and is used to calculate the adsorption capacity and rate [25]. The

Temkin model explains the interaction of the adsorption process with chemical reactions. It expresses the relationship between the interaction of adsorbate molecules on surface of adsorbent and equilibrium state of adsorption. The Temkin isotherm equation is also non-linear expression of the adsorption process and is used to calculate the adsorption capacity and rate [26]. These three models mathematically express the adsorption isotherms while addressing different aspects of the adsorption process and their interactions. The use of these models helps to understand and optimize the adsorption process. The nonlinear equations for these models are presented in equations 2, 3, and 4.

$$q_e = \frac{Q_0 b C_e}{1 + b C_e} \tag{2}$$

$$q_e = K_F C_e^{\frac{1}{n}} \tag{3}$$

$$q_e = \frac{RT}{b_T} ln\, A_T C_e \tag{4}$$

The function and plot of the isotherms are shown in Figure 5 A, and Table 1, respectively.

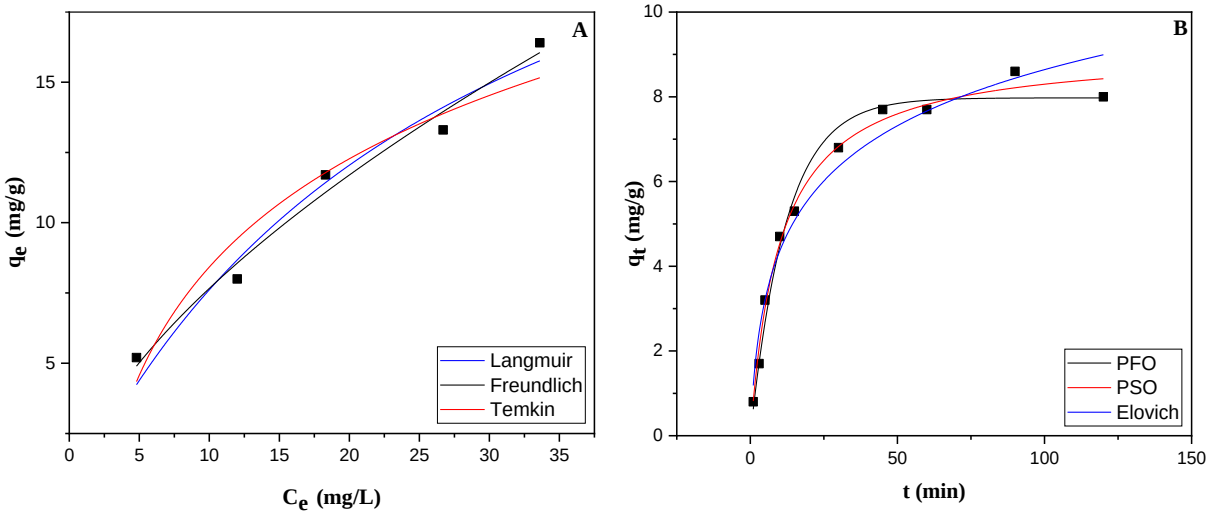

Figure 5. A. Non-linear isotherms plots B. Non-linear kinetics plots

Table 1 shows that at 41°C, langmuir isotherm model yielded maximum monolayer adsorption capacity (q_m) of 37.8 mg/g. Langmuir isotherm constant (K_L) was found to be 0.02 L/mg, with R^2 value of 0.99. From Freundlich model, K_F is an approximate indicator of adsorption capacity, while 1/n represents the strength of adsorption in the process. If n = 1, the partition between the phases does not depend on the concentration. Value of 1/n below one indicates normal adsorption, while a value above one indicates cooperative adsorption. At a temperature of 21°C, the K_F value was determined to be 1.88, the n value was found to be 1.63, and the R^2 value was calculated to be 0.982. According to the Temkin model, A_T represents equilibrium binding constant (L/g). Maximum A_T value was computed to be 0.45 at a temperature of 21°C, with an R^2 value of 0.939.

Adsorption kinetics are mathematical models that describe speed of adsorbate molecules on surface of adsorbent and change of adsorption process over time. These models are used to calculate rate of the adsorption process and the adsorption capacity [27].

Table 1. Adsorption isotherm constant

	Langmuir			Freundlich			Temkin		
°C	q_m	K_L	R^2	K_F	n	R^2	b_T	A_T	R^2
21	28.8	0.03	0.967	1.88	1.63	0.982	439.9	0.45	0.939
31	35.4	0.02	0.985	1.33	1.41	0.978	378.8	0.28	0.983
41	37.8	0.02	0.990	1.22	1.36	0.980	373.5	0.26	0.996

The pseudo first order model is kinetic model that describes rate of adsorption process. In this model, adsorption rate is proportional to concentration of molecules adsorbed to surface of the adsorbate. This model is used to calculate initial rate and rate constant in adsorption process [28]. The second order model is another kinetic model that explains speed of adsorption process. In this model, adsorption rate is proportional to square of concentration of molecules adsorbed to the surface of the adsorbate. This model is used to calculate rate constant and adsorption capacity in the adsorption process [29]. The Elovich model is another kinetic model that explains the speed of adsorption process. In this model, adsorption rate is expressed as a function of number of molecules adsorbed to surface of adsorbate and activation energy in the adsorption process. The Elovich model is used to calculate rate constant and adsorption capacity in the adsorption process [30]. These three models mathematically express the rate in the adsorption process and are used to calculate the adsorption capacity. The pseudo first order model is used to calculate initial rate and rate constant in the adsorption process, while second order model is used to calculate rate constant and adsorption capacity in the adsorption process. The Elovich model is used to calculate activation energy and rate constant in the adsorption process. The nonlinear equations for these models are presented in equations 5, 6, and 7.

$$q_t = q_e(1-e^{-k1t}) \quad (5)$$

$$qt = (k_2 q_e^2 t)/(1+k_2 q_e t) \quad (6)$$

$$qt = (1/b)ln(abt+1) \quad (7)$$

The function and plot of the isotherms are shown in Figure 5 B, and Table 2, respectively

Table 2. Adsorption kinetic constant

			Pseudo-First Order			Pseudo-Second Order			Elovich		
Particle size	**°C**	C_0	k_1	q_e	R^2	k_2	q_e	R^2	**a**	**b**	R^2
0.5>PP>0.425	21	20	0.08	7.97	0.983	0.01	9.14	0.990	1.63	0.51	0.965
0.5>PP>0.425	21	30	0.09	10.6	0.938	0.01	11.9	0.971	3.48	0.43	0.977
PP>0.25	21	30	0.29	10.2	0.817	0.03	11.0	0.942	29.8	0.65	0.976
1>PP>0.85	21	30	0.05	9.23	0.987	0.01	10.9	0.979	1.07	0.38	0.954
0.5>PP>0.425	21	40	0.14	13.1	0.845	0.01	14.1	0.910	13.6	0.45	0.935
0.5>PP>0.425	31	30	0.09	10.6	0.977	0.01	12.0	0.985	3.11	0.41	0.956
0.5>PP>0.425	41	30	0.14	10.5	0.938	0.01	11.5	0.957	6.82	0.50	0.925

.

In general, chemisorption processes can be described using the pseudo-second-order and Elovich models. The pseudo-second-order model accounts for the involvement of valency forces, such as covalent forces and ion exchange, through the sharing or exchange of electrons between the adsorbate and adsorbent. On the other hand, the Elovich model explains the kinetics of chemisorption on a heterogeneous surface of the adsorbent. After analyzing the fitted models (Figure 5B) and their corresponding parameters (Table

2), it was observed that the pseudo-second-order and Elovich models exhibited a better fit with a higher coefficient of determination (R^2) compared to the pseudo-first-order model. This suggests that chemisorption mechanisms play a significant role in the adsorption of the MG dye.

4. CONCLUSIONS

An experimental study was conducted to investigate the efficacy of PPs - a common agricultural residue - in removing MG dye from aqueous solutions. The study examined various parameters, including temperature, pH, particle size, contact time, and initial concentration, to determine their effect on the adsorption of MG onto the adsorbent. Results indicated that the loading of MG onto PP increased with initial concentration, time, and pH. The optimal contact time was found to be 120 min, with adsorption kinetics showing an initial fast phase followed by a slower equilibrium phase. Kinetic modeling of MG adsorption was performed using pseudo-first-order (PFO), pseudo-second-order (PSO), and Elovich models. PSO was found to describe the kinetics better than the other models. Based on this model, the highest R^2 value was found to be 0.99 at 21°C. The physical, chemical, elemental, and spectroscopic characteristics of the PP residue adsorbent were studied, and the findings indicate that the loading of MG may involve ion exchange and adsorption-complexation mechanisms. Equilibrium sorption studies were modeled using Temkin, Langmuir, and Freundlich isotherms, with the Langmuir model providing the best fit. Based on this model, the maximum adsorption capacity (q_{max}) at 21°C was determined to be 25.8 mg/g. However, adsorption was found to be non-endothermic in temperature experiments. Thus, while the Freundlich model was suitable at low temperatures, the Temkin model was deemed more appropriate at higher temperatures. In summary, the findings of this study demonstrate the promising capability of utilizing agricultural waste residue as a viable adsorbent for efficient removal of MG dye.

Declaration of Ethical Standards

The authors state that the materials and methods employed in this study do not necessitate ethical committee approval.

Credit Authorship Contribution Statement

All authors made equal contributions to this study.

Declaration of Competing Interest

The authors state that they do not have any known conflicting financial interests or personal relationships.

Funding / Acknowledgements

The authors acknowledge the financial support of The Scientific and Technological Research Council of Türkiye under (TUBITAK) 2209-A Research Project Support Programme for Undergraduate Students.

Data Availability

The study's supporting data is included in the article.

REFERENCES

[1] S. Sharma, A. Hasan, N. Kumar, and L. M. Pandey, “Removal of methylene blue dye from aqueous solution using immobilized agrobacterium fabrum biomass along with iron oxide nanoparticles as biosorbent,” Environmental Science and Pollution Research, vol. 25, no. 22, pp. 21605–21615,

2018. doi:10.1007/s11356-018-2280-z

[2] M. T. Yagub, T. K. Sen, S. Afroze, H.M. Ang, "Dye and its removal from aqueous solution by adsorption: A review," Advances in Colloid and Interface Science, vol. 209, pp. 172-184, 2014. doi:10.1016/j.cis.2014.04.002

[3] K.Y.A. Lin, H.A. Chang, "Ultra-high adsorption capacity of zeolitic imidazole framework-67 (ZIF-67) for removal of malachite green from water," Chemosphere, vol. 139, pp. 624–631, 2015. doi:10.1016/j.chemosphere.2015.01.041

[4] A. Elhalil, H. Tounsadi, R. Elmoubarki, F.Z. Mahjoubi, M. Farnane, M. Sadiq, M. Abdennouri, S. Qourzal, N. Barka, "Factorial experimental design for the optimization of catalytic degradation of malachite green dye in aqueous solution by Fenton process," Water Resour Ind., vol. 15, pp. 41–48, 2016. doi:10.1016/j.wri.2016.07.002.

[5] R. Selvasembian, P. Balasubramanian, "Utilization of unconventional lignocellulosic waste biomass for the biosorption of toxic triphenylmethane dye malachite green from aqueous solution," International Journal of Phytoremediation, vol. 20 no. 6, pp. 624-633, 2018. doi:10.1080/15226514.2017.1413329.

[6] M. Liu, Z. Liu, T. Yang, Q. He, K. Yang, H. Wang, "Studies of malachite green adsorption on covalently functionalized Fe3O4@SiO2–graphene oxides core–shell magnetic microspheres," J Solgel Sci Technol., vol. 82, pp. 424–431, 2017. doi: 10.1007/s10971-017-4307-1.

[7] H. A. Al-Yousef, B. M. Alotaibi, M. M. Alanazi, F. Aouaini, L. Sellaoui, A. Bonilla-Petriciolet, "Theoretical assessment of the adsorption mechanism of ibuprofen, ampicillin, orange G and malachite green on a biomass functionalized with plasma," Journal of Environmental Chemical Engineering, vol. 9, no. 1, pp 104950, 2021. doi: 10.1016/j.jece.2020.104950.

[8] B. Takam, J. B. Tarkwa, E. Acayanka, S. Nzali, D. M. Chesseu, G. Y. Kamgang, S. Laminsi, "Insight into the removal process mechanism of pharmaceutical compounds and dyes on plasma-modified biomass: the key role of adsorbate specificity." Environ. Sci. Pollut. Res., vol. 27, pp. 20500–20515, 2020. doi: 10.1007/s11356-020-08536-3.

[9] Sharma, Neetu, D. P. Tiwari, S. K. Singh, "The efficiency appraisal for removal of malachite green by potato peel and neem bark: isotherm and kinetic studies." International Journal, vol.5, no.2, pp. 84-88 2014.

[10] A. Stavrinou, C.A. Aggelopoulos, C.D. Tsakiroglou, "Exploring the adsorption mechanisms of cationic and anionic dyes onto agricultural waste peels of banana, cucumber and potato: Adsorption kinetics and equilibrium isotherms as a tool." Journal of Environmental Chemical Engineering, vol.6, no.6, pp. 6958-6970, 2018. doi: 10.1016/j.jece.2018.10.063.

[11] Ioannis Anastopoulos, George Z. Kyzas, "Agricultural peels for dye adsorption: A review of recent literature." Journal of Molecular Liquids, vol. 200, Part B, pp. 381-389, 2014. doi:10.1016/j.molliq.2014.11.006.

[12] G. El-Khamsa, H. Oualid, "Sorption of malachite green from aqueous solution by potato peel: Kinetics and equilibrium modeling using non-linear analysis method," Arabian Journal of Chemistry, vol. 9, pp. S416-S424, 2016. doi: 10.1016/j.arabjc.2011.05.011.

[13] U. Farooq, M. A. Khan, M. Athar, J. A. Kozinski, "Effect of modification of environmentally friendly biosorbent wheat (Triticum aestivum) on the biosorptive removal of cadmium (II) ions from aqueous solution," Chemical Engineering Journal, vol. 171, no. 2, pp. 400-410, 2011. doi: 10.1016/j.cej.2011.03.094.

[14] T.K. Naiya, B. Singha, S.K. Das, "FTIR study for the Cr(VI) removal from aqueous solution using rice waste," International Conference on Chemistry and Chemical Process-IPCBEE, vol. 10 pp114–119, 2011.

[15] H. Yang, R. Yan, H. Chen, D.H. Lee, C. Zheng, "Characteristics of hemicellulose, cellulose and lignin pyrolysis," Fuel, vol. 86, pp. 1781–1788, 2007.

[16] M. J. K. Ahmed, M. Ahmaruzzaman, R. A. Reza, "Lignocellulosic-derived modified agricultural waste: Development, characterisation and implementation in sequestering pyridine from aqueous

solutions," Journal of Colloid and Interface Science, vol. 428, pp. 222-234, 2014. doi. 10.1016/j.jcis.2014.04.049.

[17] E. D. Asuquo, A. D. Martin, "Sorption of cadmium (II) ion from aqueous solution onto sweet potato (Ipomoea batatas L.) peel adsorbent: Characterisation, kinetic and isotherm studies," Journal of Environmental Chemical Engineering, vol. 4, no. 4, pp. 4207-4228, 2016. doi: 10.1016/j.jece.2016.09.024.

[18] Z. Zhezi, Z. Mingming, Z. Dongke, "A Thermogravimetric study of the characteristics of pyrolysis of cellulose isolated from selected biomass," Applied Energy, vol. 220, pp. 87-93, 2018. doi: 10.1016/j.apenergy.2018.03.057.

[19] W. Qu, T. Yuan, G. Yin, S. Xu, Q. Zhang, H. Su, "Effect of properties of activated carbon on malachite green adsorption," Fuel, vol. 249, pp. 45-53, 2019. doi: 10.1016/j.fuel.2019.03.058.

[20] M.A. Al-Ghouti, R.S. Al-Absi, "Mechanistic understanding of the adsorption and thermodynamic aspects of cationic methylene blue dye onto cellulosic olive stones biomass from wastewater," Sci. Rep., vol. 10, pp. 15928, 2020. doi: 10.1038/s41598-020-72996-3.

[21] C. Silva, B. Gama, A. Gonçalves, J. Medeiros, A. Abud, "Basic-dye adsorption in albedo residue: effect of pH, contact time, temperature, dye concentration, biomass dosage, rotation and ionic strength," J. King Saud. Univ. Eng. Sci. vol. 32 no. 6, pp. 351–359 2019. doi: 10.1016/j.jksues.2019.04.006.

[22] S. Ben-Ali, I. Jaouali, S. Souissi-Najar, A. Ouederni, "Characterization and adsorption capacity of raw pomegranate peel biosorbent for copper removal, Journal of Cleaner Production," vol. 142, no. 4, pp. 3809-3821, 2017. doi: 10.1016/j.jclepro.2016.10.081.

[23] M. A. Al-Ghouti, D. A. Da'ana, "Guidelines for the use and interpretation of adsorption isotherm models: A review," Journal of Hazardous Materials, vol. 393, pp. 122383, 2020. doi: 10.1016/j.jhazmat.2020.122383.

[24] H. Swenson, N. Stadie, "Langmuir's theory of adsorption: a centennial review," Langmuir, vol. 35 no. 16, pp. 5409–5426, 2019. doi: 10.1021/acs.langmuir.9b00154.

[25] N. Ayawei, A. N. Ebelegi, D. Wankasi, "Modelling and Interpretation of Adsorption Isotherms," Hindawi Journal of Chemistry, vol. 11 pp. 3039817, 2017. doi: 10.1155/2017/3039817.

[26] M. Vadi, A. Mansoorabad, M. Mohammadi, N. Rostami, "Investigation of Langmuir, Freundlich and temkin adsorption isotherm of tramadol by multi-wall carbon nanotube," Asian J. Chem., vol. 25 no. 10, pp. 5467–5469, 2013. doi: 10.14233/ajchem.2013.14786.

[27] J. Wang, X. Guo, "Adsorption kinetic models: Physical meanings, applications, and solving methods," Journal of Hazardous Materials, vol. 390, pp. 122156, 2020. doi: 10.1016/j.jhazmat.2020.122156.

[28] G. Ersan, Y. Kaya, M.S. Ersan, O.G. Apul, T. Karanfil, "Adsorption kinetics and aggregation for three classes of carbonaceous adsorbents in the presence of natural organic matter," Chemosphere, vol. 229, pp. 514–524, 2019. doi: 10.1016/j.chemosphere.2019.05.014.

[29] G. Sabarinathan, P. Karuppasamy, C.T. Vijayakumar, T. Arumuganathan, "Development of methylene blue removal methodology by adsorption using molecular polyoxometalate: kinetics, thermodynamics and mechanistic Study," Microchem. J., vol. 146, pp. 315–326, 2019. doi: 10.1016/j.microc.2019.01.015.

[30] C. Lin, W. Luo, T. Luo, Q. Zhou, H. Li, L. Jing, "A study on adsorption of Cr (VI) by modified rice straw: characteristics, performances and mechanism," J. Clean. Prod., vol. 196, pp. 626–634, 2018. doi: 10.1016/j.jclepro.2018.05.279.